Islamic Azad University

Journal of

Optoelectronical Nanostructures

Spring 2024 / Vol. 9, No. 2

Research Paper

Effects of Effective Layer Thickness, Light Intensity and Electron-Hole Pair Separation Distance on The Performance of Organic Bulk Heterojunction Solar Cells

Aliasghar Ayobi[*,1]

[1]Department of Physics, Bojnourd Branch, Islamic Azad University, Bojnourd, Iran

Received: 20 Feb. 2024
Revised: 28 Mar. 2024
Accepted:25 Apr. 2024
Published: 15 Jun. 2024

Use your device to scan and read the article online

Keywords:
Organic Photovoltaic (OPV), Bulk Hetero-Junction (BHJ), Open Circuit Voltage, Short Circuit Current

Abstract

In this paper the influence of different parameters such as active layer thickness, light intensity and charge separation distance on the photocurrent-voltage, short circuit current density (J_{sc}) and open circuit voltage (V_{oc}) characteristics in MEH-PPV:PCBM BHJ devicesis studied. For this purpose, the numerical continuum modelbased on drift-diffusion approximation is used. The J-V characteristics of MEH-PPV:PCBM BHJ devices under illumination change considerably with varying the active layer thickness from 40nm to 280nm. In these devices, as the active layer thickness increases from 40 nm to 120 nm the short-circuit current density increases dramatically. The open circuit voltage (V_{oc}) is partially affected by varying the active layer thickness. In these devices, as the light intensity increases, the current density would increase at low voltages. Also, as the charge separation distance “a” increases, The exciton dissociation rate ($k_{diss}n_{exc}$) and current density would decrease.

Citation: Aliasghar Ayobi. Effects of effective layer thickness, light intensity and electron-hole pair separation distance on the performance of organic bulk heterojunction solar cells. **Journal of Optoelectronical Nanostructures. 2024; 9 (2): 22- 46.**
DOI: 10.30495/JOPN.2024.32692.1305

***Corresponding author:** Aliasghar Ayobi
Address: Department of Physics, Bojnourd Branch, Islamic Azad University, Bojnourd, Iran. **Tell:**09151863185 **Email:** auobi_ali@yahoo.com

1. INTRODUCTION

During the last decade, much researches have been concentrated on organic photovoltaic (OPV) devices due to their many beneficial properties including low cost for material and fabrication equipment, lightweight, flexibility, renewable energy sources and room temperature solution process deposition. However, owing to their low power conversion efficiency (PCE), intensive research is done to improve their efficiency using new materials and device structures [1-3]. Bulk hetero-junction (BHJ) structure consists of an interpenetrating network of n-type (donor) organic material and p-type (acceptor) organic materials. Organic conducting materials have attracted much attention for use in organic BHJ solar cells due to their optical, electronic and mechanical properties and charge transfer between donor and acceptor organic materials [4-7]. However, these materials have the following limitations: the big band gap of these materials limits the ability to capture photons with wavelengths higher than the wavelength of sunlight and the very low charge carrier mobility of these materials leads to poor conductivity and cuts down the output power efficiency. Also, due to the possibility of changing properties of organic materials such as molecular mass, energy band gap and optical absorption, the performance of OPV_S can be improved. It is possible to fabricate organic solar cells with higher variability and flexibility because a variety of novel absorber and transporter materials has been synthesized in the last decade. It has been reported that the power conversion efficiency of organic BHJ solar cells can be exceed than 11% [8,9].

For created electron-hole pairs after photo absorption, it might occur each of the following processes: Electrons and holes can be collected by the cathode or anode or recombine with each other. Cathode (anode) is as a right electrode for electron (hole) and anode (cathode) is as a wrong electrode for electron (hole). Only the electrons (holes) collected by the right electrode contribute to the photocurrent. In this paper considering ohmic contacts, charge carriers collected by wrong electrode are neglected and the most important factor for limiting the solar cell efficiency is charge carrier recombination. Recombination of each electron can occur with the photo-generated holes (photo-carrier recombination) or diffused holes from the anode (dark carrier recombination). In the short-circuit condition due to the high built-in potential, the dark carriers cannot diffuse in to the bulk of organic semiconductor and are concentrated in the organic-metal interface while in the open-circuit condition due to the existence of a flat energy band, the dark carriers diffuse inside the bulk.

The replacing of Ohmic contacts with Schottky contacts leads to the changes of the solar cell behavior. So that dark carriers are removed due to the energy

barriers and the recombination is related to the photo-carriers. With increasing the carrier mobility, the solar cell efficiency increases due to the faster motion of carriers toward the electrode under built-in potential. In fact for schottky contacts, the collection of carriers with wrong electrode is not negligible since in this case there are not interface charge carriers while for ohmic contacts, electrons (holes) cannot reach to the high work function anode (cathode) due to the existence of high density of holes (electrons) around the interface between the effective material and anode (cathode). Therefore recombination will occur in the effective medium before reaching the interface.

The performance of organic solar cells is characterized with several device parameters.Since experimentally device optimization for obtaining highest efficiency is a challenging task, for this purpose the simulation based studies have key importance and despite a wide range of models and numerical simulations for OPVs, it is necessary to quantitatively describe the bulk and interface processes in these devices.During the last two decades, extensive researches have been done to investigate the physical mechanismsofconverting light into electricity in OPV_S through the use of optical and electrical models for these devices.The most important subjects under investigation in these devices despite the progress in device physics are as follows: the origin of open circuit voltage and its dependence to light intensity and temperature, limits of the conversion efficiency, and origin of the recombination [10-12]. The physical mechanisms related to the temperature dependence of V_{oc} are not fully clear. This temperature behavior can be related to thetemperature dependence of built-in voltage [13].

The efficiency oforganic BHJ solar cell is affected by four processes as follows: the absorption of photons and creation of excitons, exciton diffusion to the donor-acceptor interface, exciton dissociation to the free charge carriers in the hetero-junctions, and carrier transport toward the electrods [14]. In the organic BHJ solar cells, exciton dissociation is well done due to the large amounts of charge separation interfaces. Also for active layer thickness larger than 200 nm, the photon absorption reaches 90% [15]. Polymer photovoltaic devices with bulk-heterojunction (BHJ) structure have the highest power conversion efficiency. This isdue to the high surface contacts for charge separation and interpenetrating network for efficient charge transport [16-19]. In order to describe photovoltaic processes in OPV_S, one can use either continuum or microscopic (discrete) model.Microscopic models based on Monte Carlo (KMC) simulations are used to study various processes in OPV_S, including recombination rate-dependent efficiency, charge injection, interfacial recombination, interaction between charge carriers and electrodes, and etc [20-23]. However, the main problem of the KMC method is its high computational

cost. In this paper the Continuum modelsbased on the drift-diffusion approach are used as a useful computational method to describe the performance of the organic BHJ solar cells based on the MEH-PPV: PCBM [24, 25].

2. MODEL AND EQUATIONS

In this paper, the physical processes of the organic BHJ solar cells such as, photocurrent-voltage characteristic are investigated by means of theoretical methods based on drift-diffusion approximation and a simulation tool ATLAS-SILVACO package. For this purpose the influence of different parameters such as active layer thickness, light intensity and charge separation distance on the photocurrent characteristics, short circuit current (I_{sc}) and open circuit voltage (V_{oc}) in MEH-PPV:PCBM BHJ devices is studied with a numerical device model.

In this model, the effective material approximation is considered for drift-diffusion simulations, in which any real interface between acceptor and donor materials are removed from simulation and the blend is considered as a single homogeneous material.In the effective medium approximation the ionization potential (IP) which defines the valance state energy (hole transport level) of the film is determined by the highest occupied molecular orbital (HOMO) level of the donor. Also the electron affinity (EA) which defines the conduction state energy (electron transport level) is determined by the lowest unoccupied molecular orbital (LUMO) level of the acceptor. The energy gap of effective material(E_g^{DA}) is defined as difference between these levels (figure 1). The main advantage of the effective medium approach is possibility of one –dimensional simulation of single layer BHJ device located between two metal contacts [26-35]. Moreover in this study, several approximations are considered as follows: parabolic density of states similar to what is considered for inorganic crystalline materials, space charge effects, recombination effect, ohmic contacts for charge collection, poll-Frankel mobility models, and neglecting losses due to exciton quenching [36, 37].

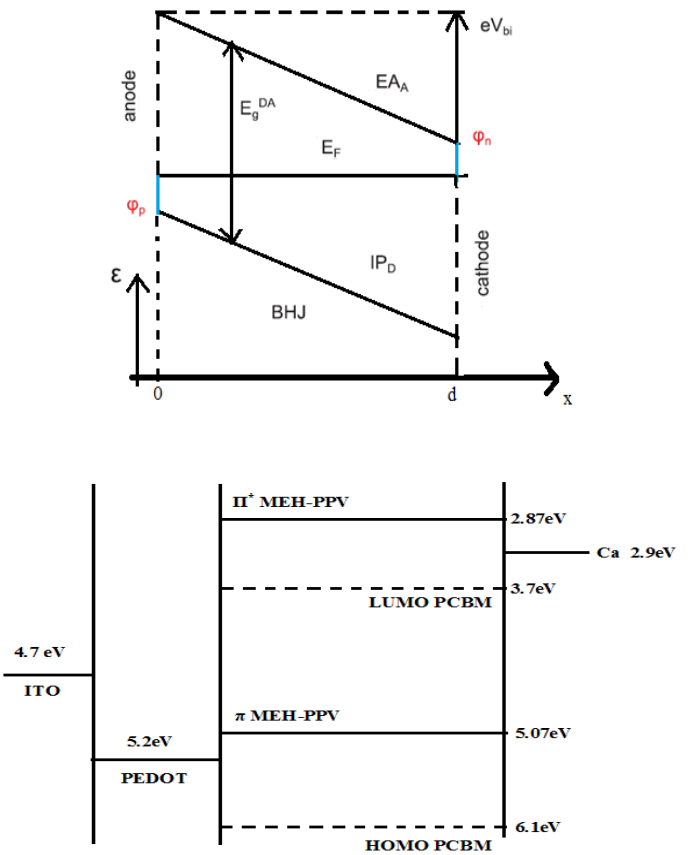

Fig.1.(a) A bulk hetero-junction (BHJ) as effective medium between two metal contacts and (b) A schematic showing energy levels of materials used in the device structure.

A. Optical absorption and exciton generation

In order to enhance the efficiency of organic solar cells it is necessary to understand all processes from photon absorption to photocurrent density (J_{ph}) extraction defined as the difference between current density under illumination (J_{illum}) and current density under dark (J_{dark}). Photocurrent in BHJ solar cells and other pin-type solar cells depends on the internal electric field and applied voltage (V) [38-40]:

$$J_{Ph}(V) = J_{illum}(V) - J_{dark}(V) \quad (1)$$

For organic BHJ solar cells, the sign of the photocurrent density changes at the compensation voltage V_0 defined as $J_{Ph}(V_0) = 0$.
The steps of converting light into electricity (photocurrent generation) in an OPV are as follows:
In the first step, transferred light to the organic compound through a transparent or semi-transparent contact (ITO, FTO, PEDOT, MoO3) is absorbed in the donor or acceptor material and leads to the excitons generation. In the second step, these excitons diffuse towards the donor-acceptor (polymer-fullerene) interface and dissociate in this interface. This dissociation leads to the formation of a geminate pair of a hole at the donor and an electron at the acceptor. These electron-hole pairs are bounded by the strongly coulomb interactions because of the low dielectric constants of the organic materials. In the final step for generation of a photocurrent, these bounded electron-hole (e-h) pairs are dissociated into free charge carriers with applying the electric field and move toward the electrodes before recombination [20, 41,42].
In some models, it is assumed that photon absorption directly creates free electrons and holes, which is approximated more than the real value, because some excitons cannot split into free charge carriers. These losses are named as exciton quenching [20, 43, 44]. However, the most important process limiting charge current is the recombination of electron-hole pairs. This recombination is characterized by a Langevin rate in which the recombination rate constant is related to electron and hole mobilities in the organic blend. The mobility of charge carriers is included in the recombination as a dominant factor to limit the efficiency of organic BHJ solar cells. In the limit of low mobility, due to the accumulation of charge carriers inside the bulk, the recombination increases while in the limit of high mobility, the recombination decreases due to the faster motion of charge carriers toward the contacts. Therefore a higher mobility leads to the improvement of the OPVs efficiency [26-30, 45-47]. Due to the typical dimension of the device (20 to 300nm) which is comparable with the wavelength of the visible incident light, the interference effects in effective medium lead to the formation of standing waves. Therefore it is not possible to apply the simple Beer-Lambert exponential decay of light intensity for this simulation. For this purpose, transfer matrix method and constant production rate are used to describe the photo-absorption and exciton generation in the simulation of a complete OPV in literature. In this manuscript a constant production rateis used for describing photo-absorption and exciton production [21-25]. Also it is assumed that an exciton is generated for each of the absorbed photons.

B. Exciton dissociation

The generated excitons after light absorption diffuse inside the absorbing material until reach to the interface between donor and acceptor materials and dissociate to their elementary charges. However dissociation will occur only if the average distance between the generation point of the excitons and the donor-acceptor interface is in the limit of the exciton diffusion length. In order to solve this problem, the acceptor and donor materials are mixed as a complex blend to form the active layer model (effective material model). In this model, due to the remove of real interface between donor and acceptor materials, the exciton diffusion equation is not included. However the exciton splitting/recombination rate is considered as the dissociation efficiency. With considering efficient splitting mechanism that in which every exciton produces an electron-hole pair it is possible to directly communication of the free carrier drift-diffusion equations to the exciton generation. In practice, the efficient splitting mechanism is not true and a part of the excitons quench before reaching to the donor-acceptor interface. Therefore in the steady state condition, the balance between the process of exciton splitting and its recombination leads to the electron-hole pair generation.

The Onsager-Braun model that widely is used in OPVs device modeling, can be used for this electron-hole pair generation rate. In this model the influence of the electric field (F), distance between the bound charges of the exciton (x) and temperature (T) is considered on the probability of the exciton dissociation (p(x,F,T)) [48]:

$$p(x,F,T) = \frac{k_d(x,F,T)}{k_d(x,F,T)+k_r} \quad (2)$$

In this equation k_r and k_d denote the rate of exciton relaxation to the ground state and the dissociation rate respectively:

$$k_d(x,F,T) = \frac{3\gamma}{4\pi x^3}\exp\left(-\frac{U_b}{k_B T}\right)\frac{J_1(2\sqrt{-2b})}{\sqrt{-2b}} \quad (3)$$

Withγ as Langevin bimolecular recombination rate constant, $U_b = \frac{q^2}{(4\pi\varepsilon_r\varepsilon_0 x)}$ as exciton binding energy, J_1 as the first order Bessel function and $b = \frac{q^3 F}{(8\pi\varepsilon_r k_B^2 T^2)}$ as field parameter. In these equations, q denotes the electronic charge,ε_r denotes the material's dielectric constant, $\varepsilon_0$denotes the permittivity of free space and $k_B$denotes the Boltzmann's constant.

In disordered polymer systems, the charge-separation distance is not constant. Therefore, the overall exciton dissociation probability is optained with using a spherically averaged Gaussian distribution as follows [49]:

$$P(F,T) = \frac{4}{\sqrt{\pi}a^3}\int_0^\infty p(x,F,T)x^2 e^{-\left(\frac{x}{a}\right)^2} dx \quad (4)$$

In this equation, parameter "a" denotes the charge-separation distance in the conditions that the probability of the Gaussian function is maximum value.
Of course, because of the controvercial presecnce of the long range electric field within the effective medium, there are doubts about the accuracy of this model to describe exciton dissociation in the effective medium approximation.Therefore, several authors with neglecting drift mechanism have considered a completely diffusion driven mechanism for charge transport in effective medium. However, due to the presence of the electric field in donor-acceptor interface one can assume that in the limit of the effective medium, this interface electric field which is the reason of the exciton splitting is substituted with a bulk electric field.

C. Basic equations

This simulation is based on the Drift diffusion equations which can be used to describe the free charge transport in organic materials. In this model, The electron (J_n) and hole (J_p) current densities are related to the carrier densities (n,p) and the electrostatic potential ($\Psi(x)$):

$$J_n = -qn\mu_n \frac{\partial}{\partial x}\Psi + qD_n \frac{\partial}{\partial x} n \quad (5)$$

$$J_p = -qp\mu_p \frac{\partial}{\partial x}\Psi - qD_p \frac{\partial}{\partial x} p \quad (6)$$

In these equations, q is elementary charge,μ_n and μ_p are the electron and hole mobility respectively and D_n and D_p are the electron and hole diffusion coefficients respectively which are characterized through the Einstein relation with T as absolute temperature and k_B as Boltzmann's constant:

$$D_n = \mu_n \frac{k_B T}{q} \quad (7)$$

$$D_p = \mu_p \frac{k_B T}{q} \quad (8)$$

The carrier densities in thermal equilibrium condition are given as:

$$n = N_c \exp\{-[E_c - q\Psi(x) - E_F]\}\beta \quad (9)$$

$$p = N_v \exp\{-[E_F + q\Psi(x) - E_V]\}\beta \quad (10)$$

With N_c and N_v as the effective densities of states (DOS) of LUMO and HOMO respectively,$\beta = \frac{1}{k_B T}$, E_c and E_v as the energy of the conduction band (LUMO level) and valance band (HOMO level) respectively and E_F as the Fermi level.
Drift-diffusion equations are coupled to the continuity equation for charge conservation and poisson equation to include the electrostatic potential:

$$\frac{\partial^2}{\partial x^2}\Psi(x) = \frac{q}{\varepsilon}[n(x) - p(x) + N_D^+ - N_A^-] \quad (11)$$

$$\frac{\partial}{\partial x}J_n(x) = -q[G - R_n] \quad (12)$$

$$\frac{\partial}{\partial x}J_p(x) = q[G - R_p] \quad (13)$$

The Poisson equation relates the electrostatic potential $\Psi(x)$ to the electron ($n(x)$) and hole ($p(x)$) densitiesso that, N_A^- and N_D^+ are ionized acceptor and donor densities respectively, q is the elementary charge and ε is the dielectric constant. In continuity equations, $J_n(x)$ and $J_p(x)$ are the electron and hole current densities respectively, G is defined as the optical generation rate of free electron-hole pairs from exciton dissociation and $R_n(R_p)$ is the total recombination rate of electrons (holes).

The charge transport in disordered organic materials is described conventionally by Poole-Frankel (PF) type field dependent hopping mobility model. According to this conventional model, at low electric field limit, carrier mobility is dependent to the temperature only but with increasing the applied electric field, it will be dependent to the applied electric fieldas follows:

$$\mu = \mu_0(T)\exp(\sqrt{E/E_0}) \quad (14)$$

Where $\mu_0(T)$, $E=-d\Psi/dx$ and E_0 are the mobility in the limit of zero field, electric field and the characteristic field of the materials respectively. Empirically, the temperature dependences of the field activation factor ($\gamma(T) = \frac{1}{\sqrt{E_0}}$) and $\mu_0(T)$ is often found to be well described by:

$$\mu_0(T) = \mu_0^* \exp\left(-\frac{\Delta}{kT}\right) \quad (15)$$

$$\gamma(T) = B\left(\frac{1}{kT} - \frac{1}{kT_0}\right) \quad (16)$$

Where Δ(effective activation energy) =0.5ev, T_0=500k and the mobility in the limit of zero field and infinite temperature (μ_0^*) and B are separate adjustable parameters for electrons and holes [50, 51].

In literature, the direct recombination rate is used as dominant mechanism for describing recombination in most organic BHJ solar cells:

$$R_{n,p} = \gamma(np - n_i^2) \quad (17)$$

In this equation γ and $n_i = \sqrt{N_c N_v}\exp[-\frac{E_g}{2k_B T}]$ is recombination constant and intrinsic charge carrier density respectively. According to the Langevin theory γ is given as follows:

$$\gamma = \frac{q(\mu_n+\mu_p)}{\varepsilon_0\varepsilon_r} \quad (18)$$

With $\varepsilon_0\varepsilon_r$ as the permittivity of the material [26, 44, 52, 53]. The planar OPVs devices under investigation in this manuscript have very small thickness, therefore only one spatial dimension (x) is considered.

In equations 12 and 13, the local exciton density n_{exc} is coupled to drift diffusion equations characterizing free charge carrier transport through the $G=k_{diss}n_{exc}$. With neglecting exciton transport in BHJ devices, this local exciton density is calculated through a local rate equation:

$$G_{R(n,p)} + G_{optical} = k_{dec}n_{exc} + k_{diss}n_{exc} \quad (19)$$

In this equation, $G_{optical}$ and $k_{diss}n_{exc}$ describe the constant generation rate of excitons with respect to the position through the sunlight absorption and the exciton dissociation rate respectively, $k_{dec}n_{exc}$ describes the exciton recombination rate through the radiative and non-radiative processes and $G_{R(n,p)} = R_{n,(p)}$ is the generation rate of excitons equal to the free electron-hole pair recombination process ($R_{n,(p)}$).

D. Organic-metal interface and charge extraction

In the final step of OPVs performance, the free charge carriers must be collected with the contacts. The open circuit voltage of the OPV is controlled by the work-functions of the materials composing the two contacts. Therefore the investigation of contact/effective medium interface is an important factor. There are several models for organic/metal interfaces in contactsthat in which the presence of trap states at the interfaces are considered to influence the charge injection from the contact into the organic layer. However these trap states have little effect on the extraction of photo-generated carriers in the organic/metal interfaces of OPVs and can be neglected. With considering a constant vacuum level between organic layer and metal interface and neglecting the dipole shift related to the charge accumulation at the interface, only the work-function of the metal at the contacts affects on the energy alignment between energy gap and metal Fermi energy. In this simulation study a BHJ device is considered to be sandwiched between two metal contacts as anode and cathode that are located at x=0 and x=d respectively (figure1(a)). Also, a simple temperature dependent injection model (thermionic injection model) is used for describing the current or the charge carrier densities at the contacts [20, 54]:

$$J_{int} = (n - n_0)v = [n - N_c \exp\left(-\frac{\varphi_n}{k_B T}\right)]\, v \quad (20)$$

In this equation ν ($\nu \geq 10^6 cm/s$) and $n_0$represent the interface recombination velocity and the equilibrium charge carrier density respectively with N_c as effective density of states and φ_n as injection barrier for electrons defined as

difference between the charge transport levels and the metal work function. For organic material with parabolic density of states similar to the inorganic material with standard Schottky model this velocity is related to the effective mass of the semiconductor. The metal/organic contact of BHJ solar cell, is considered to be a sufficient majority charge carrier extraction. In this case $s \to \infty$ and thus the contacts are in equilibrium and all excess charge carriers are instantaneously extracted ($n(d)=n_0(d)$ and $p(0)=p_0(0)$). If some insulating layer be placed between metal and active material, the majority carrier extraction velocity will reduced. This topic is not discussed in this manuscript.

Often, the concepts "majority" and "minority" are related to the doped layers. In this manuscript, these concepts are related to the concentrations of charge carriers in active layer of BHJ device close to the contacts. Therefore electrons and holes are considered as majority charge carrier at the cathode and anode respectively provided that $\varphi < \frac{E_g^{DA}}{2}$. The equilibrium densities of electrons at the anode and holes at the cathode are very low due to the large injection barrier as $(E_g^{DA} - \varphi_p)$for electrons at the anode and $(E_g^{DA} - \varphi_n)$ for holes at the cathode. Therefore these carriers are defined as the minority.

The built-in potential (V_{bi}) is defined as the difference between anode and cathode work functions and according to the Fig.2 can be written as follow:

$$V_{bi} = E_g^{DA} - \varphi_n^{cathode} - \varphi_p^{anode} \quad (21)$$

To obtain a proper solution for the problem it is necessary to apply the appropriate boundary condition. If the work function of the anode (PEDOT:PSS) lies below the HOMO level of MEH-PPV and the work function of cathode (Ca) lies above the LUMO level of PCBM it would be possible to consider the Ohmic boundary conditions (Figure 1(b)).

In this case, for the anode located at x=0:

$$p(0) = N_V \quad (22)$$

$$n(0) = N_C \exp(-\frac{E_g}{k_B T}) \quad (23)$$

And for the cathode located at x=L:

$$n(L)=N_C \quad (24)$$

$$p(L) = N_V \exp(-\frac{E_g}{k_B T}) \quad (25)$$

Another boundary condition is applied to the electric potential in the short circuit condition as follows:

$$\Psi(0) = \Psi(L) = 0 \quad (26)$$

The necessary parameters for this simulation are given in table 1[55-58].

TABLE 1. The quantities used in device simulation.

Quantity	Symbol	Value
Dielectric constant	ε_r	3.4
Relaxation rate	k_r	5×10^6 1/s
Exciton charge-separation distance	a	1.3 nm
Electron transport level (PCBM LUMO)	E_c	3.7 eV
Electron effective density of states	N_c	$5.3\times 10^{25} 1/m^3$
Hole transport level (MEH-PPV HOMO)	E_v	5.07 eV
Hole effective density of states	N_v	$4.2 \times 10^{25} 1/m^3$
Electron zero-field mobility	$\mu_{n,0}$	$7 \times 10^{-8} \frac{m^2}{vs}$
Electron Poole-Frenkel field parameter	$F_{n,0}$	1×10^9 v/m
Hole zero-field mobility	$\mu_{p,0}$	$9 \times 10^{-9} \frac{m^2}{vs}$
Hole Poole-Frenkel field parameter	$F_{p,0}$	4×10^7 v/m

3. RESULTS AND DISCUSSIONS

The generation rate of bound electron-hole pairs through the absorption of light in the active layer is related to the distance exponentially. In this manuscript since the devices are very thin, therefore the assumption of uniform generation of bound electron-hole pairs does not give rise to serious inconsistencies and a homogenous rate is considered for this generation. In photovoltaic devices, the short circuit current is related to light absorption. For this reason, it is possible to describe the oscilatory nature of short circuit current in term of optical effects. Figures 2, 3 and 4 show the calculated current density-voltage characteriatics at various active layer thickness and short circuit current density-active layer thickness and open circuit voltage-active layer thickness charactetistic for BHJ devices with MEH-PPV: PCBM as active layer.

In the first step, the reference BHJ device with the structure of ITO/PEDOT/MEH-PPV:PCBM/Ca is simulated by varying the thickness of active layer (MEH-PPV:PCBM) from 40nm to 280nm.The calculated current density-voltage characteristics for BHJ devices with different active layer thickness are shown in Fig.2. Figure 2(a) shows the J-V curves in a linear plot

calculated under illumination at a light intensity of150 mW/cm^2 under constant photo-generation rate. In this figure, as the active layer thickness increases from 40 nm to 280 nm, the current density-voltage curves shift to higher values .The reason is related to increasing the amount of absorbed light as the active layer thickness increases. This leads to increasing of photo-generated charge carriers and current density. Also, Figure 2(b) shows the J-V curves in a log-log plot calculated under dark. As can be seen from this figure, the increasing of active layer thickness cannot lead to serious change in dark current densityexcept for 40nm to 80nm. From 40nm to 80nm the increasing of active layer thickness lead to increased dark current density.

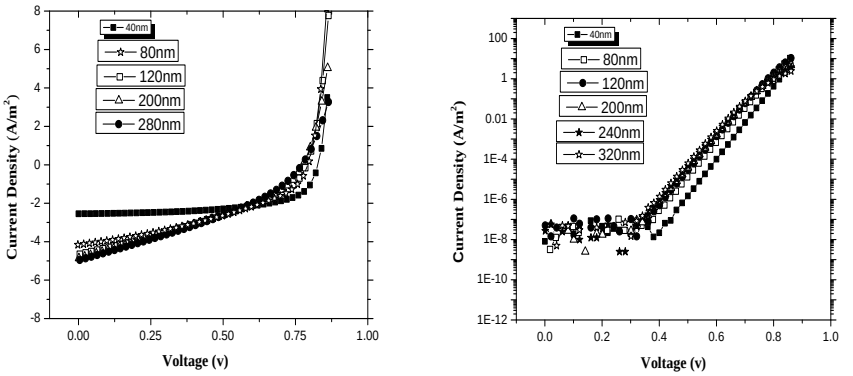

(a) (b)

Fig.2. J-V characteristics of PV devices as a function of active layer thickness (a) under illumination at a light intensity of 150 mW /cm^2 and (b) in the dark.

Figure 3 shows the effective photocurrent density (J_{ph}) as a function of the applied voltage at different active layer thicknesses, calculated by subtracting dark current from the illumination current.In this figure, as the active layer thickness increases for voltages below 0.6v, the Photocurrent increases. The reason is that as the active layer thickness increases,the absorbed light would increase which lead to increasing of photo-generated charge carriers and current density. Also in these voltages, the photocurrent-voltage curves have linearly shape which is related to zero recombination rate and direct competition between diffusion and drift current in low voltages. After a certain voltage (0.6 v), the photocurrent-voltage curves will not be linear, and increasing the thickness of active layer lead to decreasing of the light current. The reason is that, with assuming zero recombination, at higher applied voltages, all free charge carriers are extracted and photocurrents saturate to qGL. But since in this manuscript, the recombination rate is opposite to zero, therefore the simulated

photocurrent does not saturate at qGL and gradually decreases for voltages above 0.6 v.

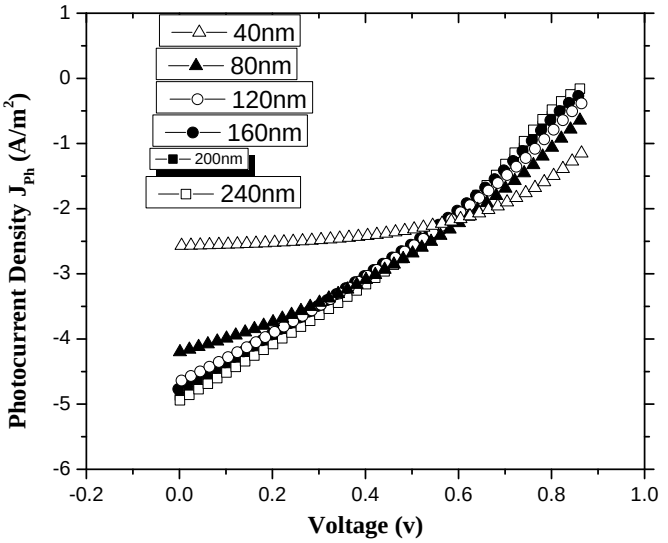

Fig.3.J_{Ph}-V characteristics of PV devices as a function of active layer thickness

.

Figure 4(a), shows the variation of the short circuit currentdensity with active layer thickness. This figure shows that as the active layer thickness increases from 40nm to 120nm, the short circuit current density increases dramatically but from 120nm to 280 nm this increasing is slower. The devices with active layer thickness of 40nm have the lowest short circuit current (J_{sc}=2.54A/m^2) and the devices with active layer thickness of 280nm have the highest short circuit current (J_{sc}=5.02 A/m^2).In photovoltaic devices, the short circuit current density depends on amount of absorbed light by the system.For layer thicknesses in the limit of the light wavelength, the interference effects of the light will play an important role in the calculations.So thatthese optical effects can lead to fluctuations in the short circuit current density. In this paper, with ignoring the interference effects, the common assumption about the exponentially decay of the light intensity among the polymer film is considered [49]. In this model, the initial light intensity in the MEH-PPV: PCBM film is related to the light transmittance from the air into this layer so that the transmittance in the glass/ ITO/PEDOT:PSS layers is obtained using the optical multilayer theory.In this

model, the fluctuating nature of the short circuit current density and current density reduction in larger thicknesses do' not occur.
Figure 4(b), shows the variation of the open circuit voltage (V_{oc}) with active layer thickness. This figure shows that V_{oc} is only marginally affected by varying the active layer thickness so that, as the active layer thickness increases from 40nm to 80nm, the open circuit voltage decreases slowly. Then from 80nm to 120nm the open circuit voltage is constant, from 120nm to 160nm this quantity decreases slowly and from 160nm to 240nm this quantity is constant. The reason of decreasing V_{oc} as the active layer thickness increases is related to the dissociation of charge carrier. In fact as the active layer thickness increases, the electrical field E decreases for a certain voltage which lead to the reduced charge carrier dissociationand reduced open circuit voltage.

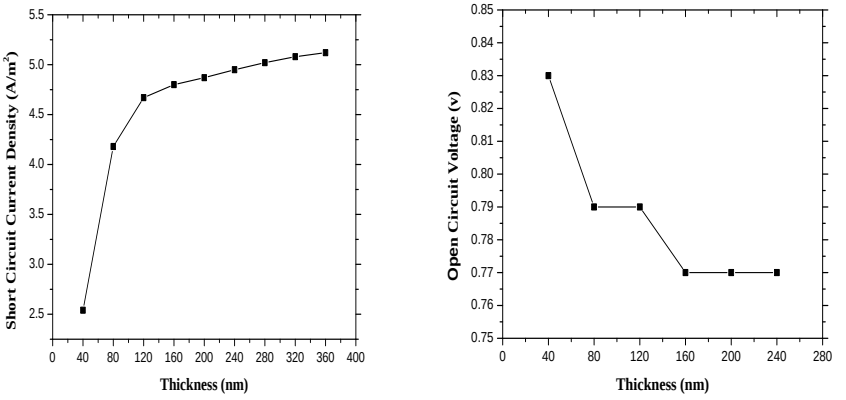

(a) (b)

Fig.4. (a) Short Circuit Current Density and (b) Open Circuit Current Density characteristics of PV devices as a function of active layer thickness under illumination.

Figure 5(a), shows the current density-voltage characteristics of BHJ devices with effective layer thickness of 200nm at different light intensity. As can be seen from this figure at low voltages, the increasing of the light intensity, lead to increased current density. As the applied voltage increases, the effect of light intensity decreases and current density-voltage curves converge. This converge near the open circuit voltage is related to the bimolecular recombination that is a dominant losses mechanism near the open circuit voltage in OPVs. Figure 5(b), shows the short circuit current density characteristics of BHJ devices in terms of illumination. This figure shows that short circuit current density has a linear dependence on incident light intensity and increases as the light intensity

increases. This variation is related to collection efficiently of photo-generated carriers prior to recombination.

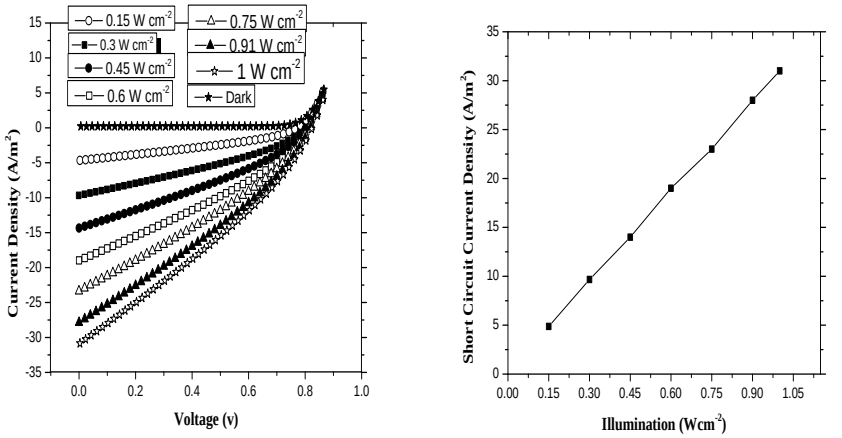

(a) (b)

Fig.5. (a) Current Density-Voltage characteristics of BHJ device at different illumination (b) Short Circuit Current Density characteristic of BHJ devices in terms of Illumination.

Figure 6, shows the current density-voltage characteristics of BHJ device with effective layer thickness of 200nm under illumination 0.45 w/cm^2 at different charge separation distance. Charge transfer states with different separation distance "a" lead to the generation of free charge carriers. The equilibrium concentration of the charge transfer states is different because this quantity depends on the separation distance "a". In fact as the separation distance "a" increases, the Coulomb binding energy $E_B(a) = \frac{q^2}{4\pi\varepsilon_0\varepsilon_r a}$ decreases and leads to a low equilibrium concentration of charge transfer states (n_{exc}). In conclusion, as the charge separation distance "a" increases, the exciton dissociation rate ($k_{diss}n_{exc}$)and current density decrease. In contrast, as the charge separation distance "a" decreases, Coulomb binding energy $E_B(a) = \frac{q^2}{4\pi\varepsilon_0\varepsilon_r a}$ increases andcarriers feel attractive forces. These attractiveforces,make the state energetically more favorable and the equilibrium concentration of the charge transfer states (n_{exc}) increases. Therefore as the charge separation distance "a" decreases, the exciton dissociation rate ($k_{diss}n_{exc}$) and current density increase.

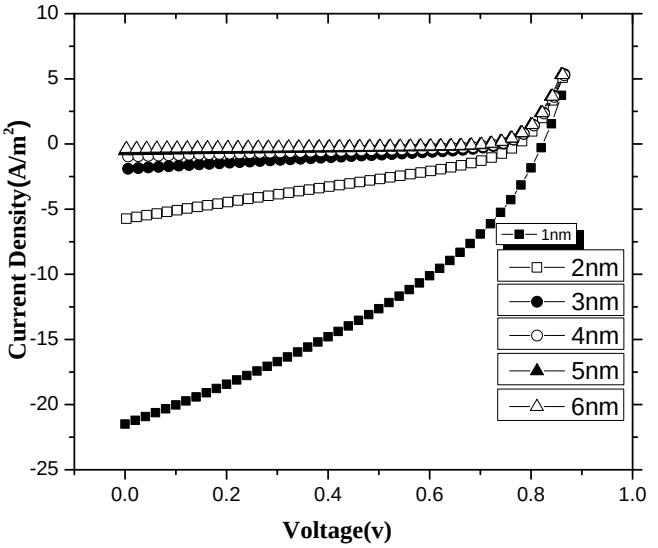

Fig.6. current density-voltage characteristics of BHJ device at different charge separation distance.

4. CONCLUSION

The J-V characteristics of MEH-PPV:PCBM BHJ devices under illumination change considerably with varying the active layer thickness from 40nm to 280nm. In the low voltage regimes, as the active layer thickness increases the Photocurrent would increase. Also in these voltages,the photocurrent increases linearly with the applied voltage. After a certain voltage, the light current changes would not be linear, and as the thickness of active layer increases, the light current would decrease.In MEH-PPV: PCBM BHJ devices, as the active layer thickness increases from 40 nm to 120 nm the short-circuit current density increases dramatically, while from 120 nm to 280 nm, these increasing is slower.Also, open circuit voltage (V_{oc}) is partially affected by varying the active layer thickness so that as the active layer thickness increases from 40nm to 80nm, the open circuit voltage decreases slowly. From 80nm to 120nm the open circuit voltage is constant, then from 120nm to 160nm this quantity decreases slowly and from 160nm to 240nm this quantity is constant.

In MEH-PPV:PCBM BHJ devices, as the light intensity increases, current density increases at low voltages, but as applied voltage increases, the effect of light intensity decreases and current density-voltage curves converge. The short

circuit current density has a linear dependence on the incident light intensity and increases as the light intensity increases. Also, as the charge separation distance "a" increases, The exciton dissociation rate ($k_{diss}n_{exc}$)and current density would decrease.

REFERENCES

[1] He, Z., et al, *Enhanced power-conversion efficiency in polymer solar cells using an inverted device structure*, Nat. Photonics 6(9), (2012) 593-597.

Available: https://doi.org/10.1038/nphoton.2012.190

[2] Dou, L., et al, *Tandem polymer solar cells featuring a spectrally matched low-band gap polymer*, Nat. Photonics 6(3), (2012) 180-185.

Available: https://doi.org/10.1038/nphoton.2011.356

[3] Li, N., et al, *Towards 15 % energy conversion efficiency: A systematic study of the solution-processed organic tandem solar cells based on commercially available materials*, Energy & Environmental Science.6 (2013) 3407-3413

Available: https://doi.org/10.1039/C3EE42307G

[4]G. Dennler, M.C.Scharber, C.J.Brabec, *Polymer-fullerene bulk-heterojunction solar cells*, Adv. Mater. 21 (2009) 1323-1338.

Available:https://doi.org/10.1002/adma.200801283

[5] M. Hasani , R. Chegell . *Electronic and optical properties of the Graphene and Boron Nitride nanoribbons in presence of the electric field.* Journal of Optoelectrical Nano Structuers.5.2 (2020) 49-64.

Available: http://jopn.miau.ac.ir/article_4218.html

[6] S. Rafiquea, S. M. Abdullaha, K. Sulaimana, M. Iwamotob, *Fundamentals of bulk heterojunction organic solar cells: An overview of stability/degradation issues and strategies for improvement*, Renewable and Sustainable Energy Reviews.84 (2018) 43–53.

Available:https://doi.org/10.1016/j.rser.2017.12.008

[7] F. A. Roghabadi, N. Ahmadi, V. Ahmadi, A. D. Carlo, K. O. Aghmiuni, A. S. Tehrani, F. S. Ghoreishi, M. Payandeh, N. M. R. Fumanid, *Bulk heterojunction polymer solar cell and perovskite solar cell: Concepts, materials*, current status, and opto-electronic properties, Solar Energy 173 (2018) 407–424.

Available:https://doi.org/10.1016/j.solener.2018.07.058

[8] W. Ma, J. Y. Kim, K. Lee, and A. J. Heeger, *Effect of the molecular weight of poly (3-hexylthiophene) on the morphology and performance of polymer bulk heteojunction solar cells*, Macromol. Rapid Commun. 28, (2007) 1776-1780.

Available:https://doi.org/10.1002/marc.200700280

[9] G. Dennler, M. C. Scharber, and C. J. Brabec, *Polymer-Fullerene bulk-heterojunction solar cells*, Adv. Mater. 21, (2009) 1323-1338.

Available: https://doi.org/10.1002/adma.200801283

[10] K. Vandewal, K. Tvingstedt, A. Gadisa, O. Inganas, J.V. Manca, *On the origin of the open-circuit voltage of polymer- fullerene solar cells*, Nat. Mater. 8 (2009) 904-909.

Available:https://doi.org/10.1038/nmat2548

[11] A. Foertig, A. Baumann, D. Rauh, V. Dyakonov, C. Deibel, *Charge carrier concentration and temperature dependent recombination in polymer-fullerene solar cells*, Appl.Phys. Lett. 95 (2009) 052104.

Available:https://doi.org/10.1063/1.3202389

[12] G. Garcia-Belmonte, P.P.Boix, J. Bisquert, M. Sessolo, H.J. Bolink, *Simultaneous determination of carrier lifetime and electron density-of-states in P3HT:PCBM organic solar cells under illumination by impedance spectroscopy*, Sol. Energy Mater. Sol. Cells 94 (2010) 366-375.

Available:https://doi.org/10.1016/j.solmat.2009.10.015

[13] A. Spies, M. List, T. Sarkar, and U.Würfel, *On the Impact of Contact Selectivity and Charge Transport on the Open-Circuit Voltage of Organic Solar Cells*, Adv. Energy Mater,(2016**)** 1601750.

Available:https://doi.org/10.1002/aenm.201601750

[14] N. Sadoogi, A. Rostami, B. Faridpak, and M. Farrokhifar, *Performance analysis of organic solar cells: Opto-electrical modeling and simulation*, Engineering Science and Technology, an International Journal.24 (2021) 229–235.

Available:https://doi.org/10.1016/j.jestch.2020.08.006

[15] S. I. Uddin, M. Tahir, F. Aziz, M. R. Sarker, F. Muhammad, D. N. Khan, and S. H. M. Ali, *Thickness Optimization and Photovoltaic Properties of*

Bulk Heterojunction Solar Cells Based on PFB–PCBM Layer, Energies.13 (2020**)**, 5915.

Available:https://doi.org/10.3390/en13225915

[16] C. Liang, Y. Wang, D. Li, X. Ji, F. Zhang, Z. He, *Modeling and simulation of bulk heterojunction polymer solar cells*,Solar Energy Materials & Solar Cells 127 (2014) 67–86.

Available:https://doi.org/10.1016/j.solmat.2014.04.009

[17] L. Jhamba, D. Wamwangi, Z. Chiguvare, *Dependence of mobility and charge injection on active layer thickness of bulk heterojunction organic solar cells: PCBM:P3HT*, Optical and Quantum Electronics.52 (2020) 245.

Available:https://doi.org/10.1007/s11082-020-02362-0

[18] W. Yang, Y. Yao, and C.Q. Wu, *Mechanisms of device degradation in organic solar cells:Influence of charge injection at the metal/organic contacts*, Organic Electronics.14 (2013) 1992–2000.

Available:https://doi.org/10.1016/j.orgel.2013.04.036

[19] C. R. Singh , C. Li , C. J. Mueller , S. Hüttner, and M. Thelakkat, *Influence of Electron Extracting Interface Layers in Organic Bulk-Heterojunction Solar Cells*, Adv. Mater. Interfaces.3 (2016) 1500422.

Available:https://doi.org/10.1002/admi.201500422

[20] A.H. Fallahpour, A.Gagliardi, F.Santoni, D. Gentilini, A.Zampetti, M.AufderMaur, and A.Di Carlo, *Modeling and simulation of energetically disordered organic solar cells*, J.Appl. Phys. 116 (2014) 184502.

Available:https://doi.org/10.1063/1.4901065

[21] M. Erray, M. Hanine, E. M. Boufounas, and A. E. Amrani, *Combined effects of carriers charge mobility and electrodes work function on the performances of polymer/fullerene P3HT:PCBM based organic photovoltaic solar cell*, Eur. Phys. J. Appl. Phys. 82 (2018) 30201.

Available:https://doi.org/10.1051/epjap/2018180070

[22] I. Hwang and N. C. Greenham, *Modeling photocurrent transients in organic solar cells*, Nanotechnology 19 (2008) 424012.

Available:https://**doi** 10.1088/0957-4484/19/42/424012

[23] W. Tress, K. Leo, and M. Riede, *Optimum mobility, contact properties, and open-circuit voltage of organic solar cells: A drift-diffusion simulation study*, Phys. Rev. B 85 (2012) 155201.

Available:https://doi.org/10.1103/PhysRevB.85.155201

[24] G. Dennler, K. Forberich, M.C. Scharber, C.J. Brabec, I. Tomis, K. Hingerl et al., *Angle dependence of external and internal quantum efficiencies in bulk-heterojunction organic solar cells*, J. Apply. Phys. 102 (2007) 054516.

Available:https://doi.org/10.1063/1.2777724

[25] R. Hausermann, E. Knapp, M. Moos, N.A. Reinke, T. Flatz, and B. Ruhstaller, *Coupled optoelectronic simulation of organic bulk-heterojunction solar cells: Parameter extraction and sensitivity analysis*, J. Apply. Phys. 106 (2009) 104507.

Available:https://doi.org/10.1063/1.3259367

[26] A. Petersen, T. Kirchartz, and T.A. Wagner, *Charge extraction and photocurrent in organic bulk hetero-junction solar cells*, Phys. Rev. B 85 (2012) 045208.

Available: https://doi.org/10.1103/PhysRevB.85.045208

[27] J.T. Shieh, C.H. Liu, H.F. Meng, S.R. Tseng, Y.C. Chao, and S.F. Horng, *The effect of carrier mobility in organic solar cells*, J. Appl. Phys. 107 (2010) 084503.

Available:https://doi.org/10.1063/1.3327210

[28] A.S. Lin and J.D.Phillips, *Drift-diffusion modeling for impurity photo-voltaic devices*, IEEE Trans. Electron Devices 56 (2009) 3168-3174.

Available: https://doi.org/10.1109/TED.2009.2032741

[29] K.Wee Shing, M. Pant, Y.A. Akimov, G. Wei Peng, and L. Yuning, *Three-dimensional optoelectronic model for organic bulk heterojunction solar cells*, IEEE J. Photovolt. 1 (2011) 84-92.

Available:https://doi.org/10.1109/JPHOTOV.2011.2163620

[30] J.D. Kotlarski, P.W.M. Blom, L.J.A. Koster, M. Lenes, and L.H.Slooff, *Combined optical and electrical modeling of polymer:fullerene bulk heterojunction solar cells*, J. Appl. Phys. 103 (2008) 084502.

Available:https://doi.org/10.1063/1.2905243

[31] W. Vervisch, S. Biondo, G. Riviere, D. Duche, L. Escoubas, P. Torchio et al., *Optical-electrical simulation of organic solar cells: Excitonic modeling parameter influence on electrical characteristics*, Appl. Phys. Lett. 98 (2011) 253306.

Available:https://doi.org/10.1063/1.3582926

[32] O. J. Sandberg, M. Nyman, and R. Osterbacka, *Effect of contacts in organic bulk hetero-junction solar cells*, Phys. Rev. Appl. 1 (2014) 024003.

Available:https://doi.org/10.1103/PhysRevApplied.1.024003

[33] R. Yahyazadeh, Z. Hashempour, *Effect of Hyrostatic pressure on optical Absorption coeffivient of InGaN/GaN of Multiple Quantum well solar cells*, Journal of optoelectronical Nano structures,6.2 (2021) 1-22

Available: https://doi.org/10.304951JOPN.2021.27941.1221

[34] M. Saleheen, S. M. Arnab, and M. Z. Kabir, *Analytical Model for Voltage-Dependent Photo and Dark Currents in Bulk Heterojunction Organic Solar Cells*, Energies.9 (2016) 412.

Available: https://doi.org/10.3390/en9060412

[35]A. Wagenpfahl, D. Rauh, M. Binder, C. Deibel, and V. Dyakonov, *S-shaped current-voltage characteristics of organic solar devices*, Phys. Rev. B. 82 (2010) 115306.

Available:https://doi.org/10.1103/PhysRevB.82.115306

[36] A.H. Fallahpour, A. Gagliardi, D. Gentilini, A. Zampetti, F.Santoni, M. Auf der maur, A. Di Carlo, *Optoelectronic simulation and thickness optimization of energetically disordered organic solar cells*, J. Comput. Electron.13 (2014) 933-942.

Available:https://doi.org/10.1007/s10825-014-0611-y

[37] F. Monestier, J.J. Simon, P. Torchio, L.Escoubas, F. Flory, S. Bailly et al., *Modeling the short-circuit current density of polymer solar cells based on P_3HT:PCBM blend*, Sol. Energy Mater. Sol. Cells.91(2007) 405-410 .

Available:https://doi.org/10.1016/j.solmat.2006.10.019

[38] T. Kirchartz, J. Mattheis, and U. Rau, *Detailed balance theory of excitonic and bulk heterojunction solar cells*,Phys. Rev. B.78 (2008) 235320.

Available:https://doi.org/10.1103/PhysRevB.78.235320

[39] G. F. A. Dibb, T. Kirchartz, D. Credgington, J. R. Durrant, and J. Nelson ,*Analysis of the Relationship between Linearity of Corrected Photocurrent and the Order of Recombination in Organic Solar Cells*,J. Phys. Chem. Lett. 2 (2011) 2407.

Available:https://doi.org/10.1021/jz201104d

[40] *S. R. Cowan, A. Roy, and A. J. Heeger, Recombination in polymer-fullerene bulk heterojunction solar cells,Phys. Rev. B.82 (2010) 245207.*

Available:https://doi.org/10.1103/PhysRevB.82.245207

[41] A.V. Nenashev, S.D. Baranovskii, M. Wiemer, F. Jansson, R. Osterbacka, A.V. Dvurechenskii et al., *Theory of exciton dissociation at the interface between a conjugated polymer and an electron acceptor*, Phys. Rev. B.84 (2011) 035210.

Available:https://doi.org/10.1103/PhysRevB.84.035210

[42] M. Wiemer, A.V. Nenashev, F. Jansson, and S.D. Baranovskii,*on the efficiency of exciton dissociation at the interface between a conjugated polymer and an electron acceptor*, Appl. Phys. Lett. 99 (2011) 013302.

Available:https://doi.org/10.1063/1.3607481

[43] C. Deibel, T. Strobel, and V. Dyakonov, *Role of the charge transfer state in organic donor-acceptor solar cells*, Adv. Mate. 22 (2010) 4097-4111.

Available:https://doi.org/10.1002/adma.201000376

[44] C. Deibel, *Charge carrier dissociation and recombination in polymer solar cells, Phys*. Status Solidi A.206 (2009) 2731-2736.

Available:https://doi.org/10.1002/pssa.200925282

[45] N.S. Christ, S.W. Kettlitz, S. Valouch, S. Zufle, C. Gartner, M. Punke et al., *Nanosecond response of organic solar cells and photodetectors*, J. Appl. Phys. 105 (2009) 104513.

Available:https://doi.org/10.1063/1.3130399

[46] G. Juska, K. Genevicius, N. Nekrasa et al., *Charge carrier transport, recombination, and trapping in organic solar cells studied by double injunction technique*, IEEE J. Sel. Top. Quantum Electron. 16 (2010) 1764-1769.

Available:https://doi.org/10.1109/JSTQE.2010.2041752

[47] R.C.I. Mackenzie, T. Kirchartz, G. F.A. Dibb, and J. Nelson, *Modeling non-geminate recombination in P3HT:PCBM solar cells*, J. Phys. Chem. C.115 (2011) 9806-9813.

Available:https://doi.org/10.1021/jp200234m

[48] A. Mahmoudloo, *Investigation and Simulation of Recombination Models in Virtual Organic Solar Cell*, Journal of Optoelectronical Nanostructures, 7.4 (2022) 1-12.

Available: https://doi:10.30495/jopn.2022.30243.1263

[49] D. Jalalian1, A. Ghadimi, A. K. Sarkaleh, *Investigation of the Effect of Band Offset and Mobility of Organic/Inorganic HTM Layers on the Performance of Perovskite Solar Cells*, Journal of Optoelectronical Nanostructures, 5.2 (2020) 65-78.

Available: https://dorl.net/dor/20.1001.1.24237361.2020.5.2.6.3

[50] S. L. M. Vanmensfoort, V. Shabro, R. J. D. Vries, R. A. J. Janssen, and R. Coehoorn, *Hole Transport in The Organic Small Molecule Material: Evidence For The Presence of Correlated Disorder*, J. Appl. Phys. 107 (2010) 113710.

Available:https://doi.org/10.1063/1.3407561

[51] A. ayobi, S.N. Mirnia, *Influence of Gaussian disorder and exponential traps on charge carriers transport and recombination in single layer polymer light-emitting diodes based on PFO as emitting layer*, Opt. Quant. Elect (2019).

Available:https://doi.org/10.1007/s11082-019-1997-3

[52] A. Pivrikas, N. S. Sariciftci, G. Juska, and R. Osterbacka, *A review of charge transport and recombination in polymer/fullerene organic solar cells*, Prog.in Photovolt.: Res. Appl. 15 (2007) 677-696.

Available:https://doi.org/10.1002/pip.791

[53] H. Hashemi , M.R. Shayesteh, M.R. Moslemi, *A Carbon Nanotube CNT – based SiGe Thin Film Solar cell structure*, Journal of optoelectronical Nano structures, 6.1(2021) 71- 86

Available:https://doi.org/10.30495/JOPN. 2021.4541

[54] J. Hwang, A. Wan, and A. Kahn, *Energetics of metal-organic interfaces: New experiments and assessment of the field*, Mater. Sci. Eng: R: Rep. 64 (2009) 1-31.

Available:https://doi.org/10.1016/j.mser.2008.12.001

[55] G. Garcia-Belmonte,*Temperature dependence of open-circuit voltage in organic solar cells from generation-recombination kinetic balance*, Sol. Energy Mater. Sol. Cells 94 (2010) 2166-2169.

Available:https://doi.org/10.1016/j.solmat.2010.07.006

[56] J. Wang,L. Xu,Y. J. Lee,M. D. A. Villa,A. V. Malko,and J. W. P. Hsu, *Effects of Contact-Induced Doping on the Behaviors of Organic Photovoltaic Devices*, Nano Lett.15 (2015) 7627−7632.

Available:https://doi.org/10.1021/acs.nanolett.5b03473

[57] M. Nyman, O. J. Sandberg, W. Li, S. Zeiske, R. Kerremans, P. Meredith, and A. Armin, *Requirements for Making Thick Junctions of Organic Solar Cells based on Nonfullerene Acceptors*, Sol. RRL.5 (2021) 2100018.

Available:https://doi.org/10.1002/solr.202100018

[58] M. Abdallaoui, N. Sengouga, A. Chala, A.F. Meftah, A.M. Meftah, *Comparative study of conventional and inverted P3HT: PCBM organic solar cell*, Optical Materials 105 (2020) 109916.

Available:https://doi.org/10.1016/j.optmat.2020.109916